

SO(3) vortices as a mechanism for generating a mass gap in the 2d SU(2) principal chiral model ¹

Tamás G. Kovács²

Department of Physics

University of California, Los Angeles

Los Angeles, California 90024-1547

Abstract

We propose a mechanism that can create a mass gap in the SU(2) chiral spin model at arbitrarily small temperatures. We give a sufficient condition for the mass gap to be non-zero in terms of the behaviour of an external Z(2) flux introduced by twisted boundary conditions. This condition in turn is transformed into an effective dual Ising model with an external magnetic field generated by SO(3) vortices. We show that having a nonzero magnetic field in the effective Ising model is sufficient for the SU(2) system to have a mass gap. We also show that certain vortex correlation inequalities, if satisfied, would imply a nonzero effective magnetic field. Finally we give some plausibility arguments and Monte Carlo evidence for the required correlation inequalities.

¹Research supported in part by NSF Grant PHY89-15286

²e-mail address: kovacs@physics.ucla.edu

1 Introduction

Two dimensional lattice spin models with a continuous non-Abelian symmetry are commonly believed to have no phase transition at finite temperature. According to the Mermin-Wagner theorem in these systems there is no ordered low temperature phase with spontaneous breakdown of the global symmetry. However this does not in itself rule out the presence of a phase transition. Indeed the 2d XY model does have a finite temperature Kosterlitz-Thouless type phase transition characterised by power-law decay of the correlation function below the critical temperature as opposed to an exponential fall-off in the high temperature phase. Two is the lower critical dimension for these models and the actual phase structure depends on the properties of the internal space in a very delicate way.

In the case of spin models with Abelian symmetries there are rigorous results concerning their low temperature behaviour. For discrete symmetries (e.g. the Ising model) there is a distinct low temperature phase with long range order while for U(1) symmetry (XY model) the presence of the KT transition has been rigorously proved [1]. Recently the exact mass gap of two dimensional spin models with various different non-Abelian symmetries has been calculated using the Bethe ansatz [2]. Scaling of the correlation function has also been observed in a high order strong coupling expansion of the $N = \infty$ $SU(N) \times SU(N)$ chiral model [3]. It would however be very desirable to have a rigorous proof of a nonzero mass gap in these models starting from first principles without any further assumptions. This would probably also contribute to our intuitive understanding of the low temperature behaviour of non-Abelian spin models.

The situation is possibly even worse in 4d gauge theories. While the U(1) theory has been rigorously proved to have a deconfining transition [4], 4d non-Abelian gauge theories are believed to remain confining down to arbitrarily small couplings but a rigorous proof of this has not yet been found. In this case we do not even have anything analogous to the Bethe ansatz solution of two dimensional spin models. In view of the analogies between 2d spin models and 4d gauge theories it would be highly desirable to have a unified physical picture of their low temperature behaviour. In particular we would like to understand confinement in gauge theories and the nonzero mass gap in 2d spin models on a similar ground.

For a few years there has been an ongoing programme to achieve this both in 4d gauge

theories [5] and in the analogous 2d spin models [6, 7]. In the present paper we report on recent progress in this direction in the context of the $SU(2)$ principal chiral model. In this model the degrees of freedom are $SU(2)$ group elements attached to the sites of a square lattice with a ferromagnetic nearest neighbour interaction $\text{tr}(U_1^\dagger U_2)$. We shall propose a mechanism that is sufficient for this system to maintain a mass gap at arbitrarily low nonzero temperature.

Instead of studying the spin-spin correlation function we shall give a sufficient condition for the mass gap to be non-zero in terms of the behaviour of an external $Z(2)$ flux introduced by twisted boundary conditions. This allows us to explicitly separate the $Z(2)$ degrees of freedom belonging to the centre of $SU(2)$ and to establish the equivalence of the $SU(2)$ spin model with a dual Ising model interacting with $SO(3)$ spins on the original lattice. We show that a non-zero magnetisation in the dual Ising model would imply a mass gap in the original $SU(2)$ model. Due to their coupling to the Ising spins, $SO(3)$ vortices will turn out to generate an external magnetic field for the Ising spins, provided certain vortex correlation inequalities are satisfied. As we shall see, up to this point all of our arguments are rigorous. Finally we shall also give some plausibility arguments and Monte Carlo evidence that the vortex correlation inequalities are indeed true. This gives a complete picture of the mass gap generation in the $SU(2)$ spin model.

The plan of the paper is as follows. In Section 2 we introduce the order parameter that we want to study, the twist. This turns out to be technically more advantageous than looking at the asymptotic behaviour of the spin-spin correlation function and it can be proved that “massive” behaviour of the twist implies the same for the correlation function. Also in Section 2 we shall briefly review some properties of the twist, in particular its high and low temperature expansion and its behaviour under duality. In Section 3 we describe the separation of $Z(2)$ and $SO(3)$ degrees of freedom and discuss the relevant $SO(3)$ vortex excitations and their dynamics. By an additional $Z(2)$ duality transformation we map the original $SU(2)$ system on a dual Ising model interacting with $SO(3)$ spins. We also rewrite the twist in this language. In Section 4 we develop an effective theory of the dual Ising system by substituting the effect of the $SO(3)$ spins with an effective Ising coupling and a magnetic field. More precisely we derive sufficient conditions for the disorder correlation in an effective Ising model to be an upper bound of the twist in the original model. These

conditions turn out to be vortex correlation inequalities containing a parameter, the effective magnetic field of the Ising system. For zero magnetic field they are easily seen to be true and in Section 5 we argue that a small but nonzero magnetic field can be chosen so that the inequalities remain true independently of the lattice size. Also in Section 5 we present some Monte Carlo evidence supporting this. In Section 6 we draw our conclusions and make some final remarks.

2 The twist as an order parameter

We want to distinguish between a massive and a massless phase in the $SU(2)$ spin model. By definition a massive phase is characterised by an exponential fall-off of the spin-spin correlation function $\langle \frac{1}{2} \text{tr} U_0^\dagger U_x \rangle$ at large distances x , where $\langle \rangle$ means expectation in the infinite volume limit. In our framework it turns out to be technically more advantageous to consider another operator, a twist winding around the lattice and its behaviour as a function of the finite lattice size.³ Since the twist has not been very commonly used as an order parameter in spin models (but see e.g. [9]), in this section we shall collect some useful results about it to make the paper self-contained.

2.1 Notation

Although we use notations that have become more or less standard in (lattice) field theory, we find it useful to include here a brief section on the notation especially for later reference.

We shall work on a finite two dimensional periodic square lattice Λ . Sites, links and plaquettes of the lattice will be denoted by s , l and p . Because of its particular simplicity we shall make use of the language of group valued forms when writing down the fields and their interactions. By a G -valued n -form we mean an assignment of G elements to oriented elementary n -dimensional simplices of the lattice. Thus e.g. a $Z(2)$ valued 2-form ω assigns a $Z(2)$ element to each plaquette and a $Z(2)$ element on a particular plaquette p will be denoted by ω_p .

³ The analogous quantity in gauge theories is the sourceless 't Hooft loop or magnetic flux free energy that has been extensively used to describe the phases of lattice gauge theories [8].

There are two useful operations that can be defined on forms, the exterior derivative “d” and its dual “d*”. They map an n -form on an $n - 1$ -form (d) and $n + 1$ -form (d*) respectively. By definition

$$(\mathrm{d}\omega)_k = \prod_{m \in \partial k} \omega_m, \quad (1)$$

where k denotes a link, m a site if ω is a 0-form; k is a plaquette and m is a link if ω is a 1-form and ∂ is the boundary operator. Similarly

$$(\mathrm{d}^*\omega)_m = \prod_{k:m \in \partial k} \omega_k, \quad (2)$$

where m is a site, k is a link if ω is a 1-form and m is a link, k is a plaquette if ω is a 2-form. Thus e.g. the curvature of a $Z(2)$ valued gauge field, a 1-form A , can simply be written as $\mathrm{d}A$. For better readability we shall always omit the parentheses so e.g. $\mathrm{d}\omega_m$ means $(\mathrm{d}\omega)_m$.

In most of the cases we shall only use $Z(2)$ valued forms the only exception being the dynamical variable in the $SU(2)$ chiral model which is an $SU(2)$ valued 0-form U_s (spins live on lattice sites). The interaction between the two spins residing at the ends, s_1 and s_2 of a given link l , can be written as $\mathrm{d}U_l = \mathrm{tr}(U_{s_1}^\dagger U_{s_2})$. This is the only case when the orientation of elementary simplices will matter.

When calculating thermal averages involving (discrete or continuous) group valued fields integration is always understood with respect to the normalised Haar measure.

2.2 Twist and duality in the Ising model

At first we look at the twist in the context of the Ising model since this will be needed later when we discuss the effective Ising model of the $SU(2)$ spin system. In the Ising model the twist is not particularly useful for distinguishing between the phases of the theory since the magnetisation provides a much simpler order parameter. Nevertheless as we shall see, the twist can also be used for this purpose.

The partition function of the Ising model is

$$Z = \prod_s \int d\sigma_s \exp\left(\beta \sum_l \mathrm{d}\sigma_l\right) \quad (3)$$

with spins $\sigma_s = \pm 1$ living on a finite periodic square lattice. Here $\int d\sigma_s$ means integration

with the normalised invariant measure⁴ on $Z(2)$, sites and links of the lattice are labelled by s and l and finally $d\sigma_l$ is the product of the two spins on the link l .

By definition the twist $\tau_i = \pm 1$ along the direction i is the operator that changes the couplings from β to $\tau_i\beta$ on a stack of links winding once around the lattice along the given direction (Fig 1). Physically $\tau_i = -1$ means that a topologically nontrivial “domain-wall” was created along the affected links. Although this domain-wall is closed, it is not a boundary of any region therefore it is impossible to transform it away by a suitable redefinition of some of the spin variables. In contrast, if the domain-wall were a boundary of a region then by a change of variables $\sigma \rightarrow \tau_i\sigma$ in the region bounded by the twist, it would be possible to cancel it and the partition sum would not depend on τ_i .

By a similar argument it can be easily seen that the twisted stack of links can be “continuously” deformed by a change of variables and the twisted partition sum does not depend on the actual location of the twisted links as long as they form a closed loop winding once around the lattice.

The two phases of the system can be characterised by its response to such a twist. Intuitively one expects that in the high temperature disordered phase, having a twist does not cost too much energy on a sufficiently large lattice. On the other hand in the low temperature broken phase where most of the spins tend to be in one direction, the free energy of the twist is expected to grow with the lattice size.

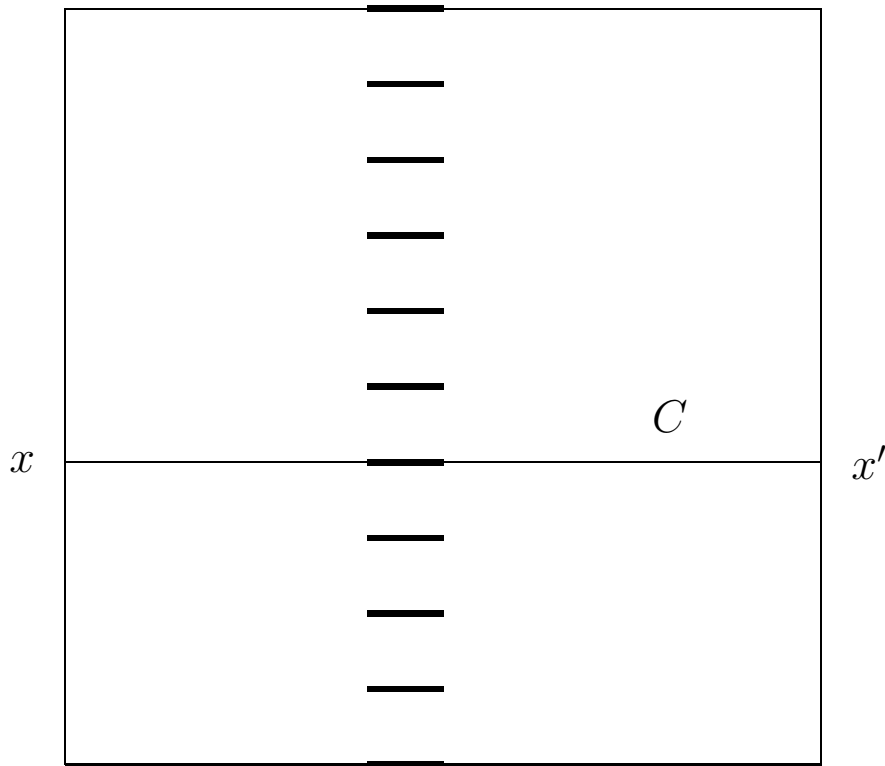
To make these ideas more precise we can consider the following observables

$$G(L) = \frac{1}{2} \frac{Z_+(L) - Z_-(L)}{Z_+(L) + Z_-(L)} \quad \text{and} \quad G^*(L) = \frac{Z_-(L)}{\frac{1}{2}(Z_-(L) + Z_+(L))}, \quad (4)$$

$$Z_{\pm}(L) = \int_{\pm} d\tau_2 Z(\pm 1, \tau_2), \quad (5)$$

where $Z(\tau_1, \tau_2)$ is the partition function with twists $\tau_1, \tau_2 = \pm 1$ in the two independent directions and L is the linear size of the lattice. (The log of) $G^*(L)$ measures how the free energy of a twist depends on the lattice size and $G(L)$ is the $Z(2)$ “Fourier-transform” of $G^*(L)$. The form of the normalisation $Z_-(L) + Z_+(L)$ in the denominator was chosen for further convenience, we could as well have used just $Z_+(L)$.

⁴Later we shall also consider continuous groups and to make the notations uniform we use the same language for discrete groups too.



$$\text{—} \quad \eta_i = -1$$

Figure 1: A twist winding around the lattice. The links on which the sign of the coupling has been reversed are shown.

At high temperature (small β) $G(L)$ decays exponentially with increasing lattice size. This can be most easily seen in the high temperature expansion. Recall that the high temperature expansion of the Ising model is the sum of closed graphs built of links of the lattice. The weight of each graph is proportional to $(\tanh \beta)^{\# \text{ of links}}$. In the presence of a twist there is an additional minus sign for each twisted link contained in the graph. Since the twist winds around the lattice, all small loops will intersect it an even number of times, so these will not contribute to $G(L)$. The lowest order contribution comes from a loop going all the way around the lattice in the direction perpendicular to the twist. The shortest such loop contains L links and is thus proportional to $(\tanh \beta)^L$. If $G(L)$ goes exponentially to

zero it means that $G^*(L)$ will go to 1 in the $L \rightarrow \infty$ limit. This is indeed what we expected, in the disordered phase the free energy of the twist remains bounded as the lattice size goes to infinity.

In the low temperature phase with the $Z(2)$ symmetry broken the behaviour of $G(L)$ and $G^*(L)$ is different. Here the free energy cost of having a twist grows linearly with the lattice size and $G^*(L)$ goes exponentially to zero while $G(L)$ goes to a nonzero constant for L large. This is certainly true for the ground state and it can also be proved in higher orders of the low temperature expansion.

Notice that the behaviour of $G(L)$ in the symmetric phase is similar to that of $G^*(L)$ in the broken phase and vice versa. This is not an accident since G and G^* are dual to one another in the following sense. The high temperature expansion of the Ising model with inverse temperature β can be identified with the low temperature expansion of a dual Ising model with spins living on the sites of the dual lattice i.e. plaquettes of the original lattice at inverse temperature β^* . This gives a mapping between the high and the low temperature regimes. It can be proved that the high temperature expansion of $G(L)$ on the original lattice is identical to the low temperature expansion of $G^*(L)$ defined in the dual system which means that $G(L)_\beta = G^*(L)_{\beta^*}$.

Finally we note that in the presence of an external magnetic field the qualitative behaviour of G and G^* is the same as in the low temperature phase. For sufficiently high temperature the high temperature expansion is convergent and the leading order exponential fall-off of $G^*(L)$ can be rigorously verified.

2.3 Twist in the $SU(2)$ spin model

It is straightforward to generalise the $Z(2)$ twist for any other spin model with a global symmetry containing $Z(2)$. In principle we could also use any element of the global symmetry group to define the twist, in spin models there is no constraint (not like in gauge theories [10]) restricting the twist to lie in the centre of the symmetry group. In this paper however we shall consider only $Z(2)$ twists.

The $SU(2) \times SU(2)$ chiral spin model is defined by the partition function

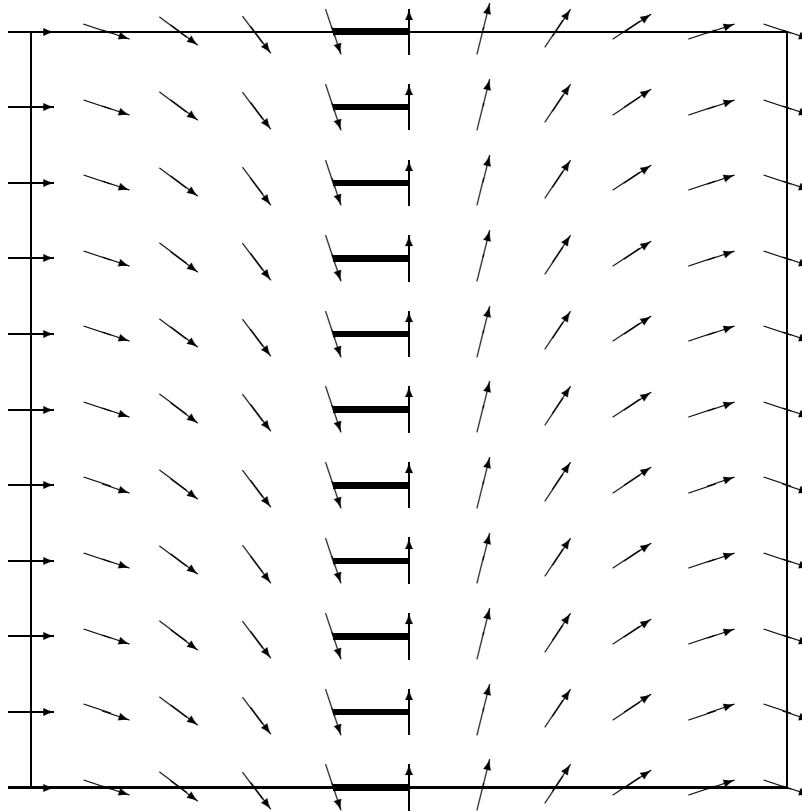
$$Z = \prod_{s \in \Lambda} \int dU_s \exp \left(\beta \sum_{l \in \Lambda} dU_l \right), \quad (6)$$

where the degrees of freedom U are $SU(2)$ group elements on the sites of the finite periodic lattice Λ and $dU_l = \text{tr}(U_s^\dagger U_{s'})$ with $[ss']$ being the boundary of the link l . The twists and the quantities $G(L)$ and $G^*(L)$ can be defined completely analogously to the Ising model.

The high temperature behaviour of these observables is qualitatively the same as in the Ising model. At low temperature however there is an important difference. In the ground state of the twisted Ising system all the spins are aligned and the energy of the twist is concentrated along a stack of links winding around the lattice parallel to the twist. On the other hand if the spins can take their values in a continuous manifold, the energy of the twist can be spread along the direction perpendicular to it.

In this case the energetically most favourable configuration has $dU_l < 0$ along the twist with the spins roughly antiparallel. The direction of the spins along the spreading direction changes gradually making half of a complete turn around the lattice (Fig 2). In the ground state neighbouring spins in the spreading direction make an angle proportional to $1/L$ costing an energy $\sim 1/L^2$ and the total energy of this configuration goes as $\sim L^2 \times 1/L^2$ on large lattices. We can see that the energy of a twist does not diverge with the lattice size, at least in the classical (zero temperature) approximation. Intuitively we expect that at nonzero temperature the twist costs even less since there is more disorder. This mechanism is analogous to flux spreading in gauge theories [11].

We saw that both in the Ising model and in the $SU(2)$ spin model the behaviour of $G(L)$ as a function of the lattice size is similar to that of the infinite volume limit of the correlation function. This motivates our choice of $G(L)$ as an indicator of the massive phase. This can be rigorously justified by proving that in the $SU(2)$ model exponential fall-off of $G(L)$ with the lattice size implies the same asymptotic behaviour of the infinite volume limit correlation function. (The proof of the analogous statement in gauge theory [8] can be easily adapted to the present case. See [12].)



— twisted links

Figure 2: The “semiclassical” ground state configuration of a twisted spin model with a continuous spin manifold. The energy of the twist can be spread in the direction perpendicular to the twist.

3 Separation of the $Z(2)$ and $SO(3)$ variables

In the previous section we saw that it is enough to prove the exponential decay of the twist $G(L)$ as a function of the lattice size in order to establish a mass gap in the $SU(2)$ spin model. Since $G(L)$ is defined in terms of a $Z(2)$ twist it will be helpful to disentangle the $Z(2)$ degrees of freedom belonging to the centre of $SU(2)$ from the rest of the system. In this Section we shall perform this task by giving a set of exact transformations that eventually map the $SU(2)$ model on a dual Ising model interacting with $SO(3)$ spins on the original lattice. We mainly follow [6] but in addition we also give a more detailed description of

the underlying dynamics of the string and vortex excitations of the $\text{SO}(3)$ system and their coupling to the Ising spins.

3.1 Gauging the $\text{Z}(2)$ symmetry

As a first step we introduce new $\text{Z}(2)$ valued link variables A_l to gauge the $\text{Z}(2)$ part of the global symmetry. To maintain the equivalence of the gauged model with the original one the gauge field A_l has to be constrained to be pure gauge by inserting a delta function $\delta(\text{d}A_p)$ for each plaquette. By definition $\text{d}A_p$ is the curvature of A_l , the product of link variables around the plaquette p and $\delta(1) = 2$, $\delta(-1) = 0$. This is however not enough to make A_l pure gauge. In addition we also have to constrain the two independent topologically nontrivial holonomies $A_{C_i} = \prod_{l \in C_i} A_l$ to be 1. Here C_1 and C_2 are two loops built of links winding around the lattice in the two independent directions.

Putting this all together the (nontwisted) partition function reads as

$$\begin{aligned} Z(1, 1) &= \prod_{s \in \Lambda} \int dU_s \prod_{l \in \Lambda} \int dA_l \prod_{p \in \Lambda} \delta(\text{d}A_p) \delta(A_{C_1}) \delta(A_{C_2}) \exp \left(\beta \sum_{l \in \Lambda} A_l \text{d}U_l \right) \\ &= \prod_{s \in \Lambda} \int dU_s \prod_{l \in \Lambda} \int d\sigma_l \prod_{p \in \Lambda} \delta(\text{d}\sigma_p \text{d}\eta_p^{-1}) \delta(\sigma_{C_1} \eta_{C_1}^{-1}) \delta(\sigma_{C_2} \eta_{C_2}^{-1}) \exp \left(\beta \sum_{l \in \Lambda} \sigma_l |\text{d}U_l| \right) \end{aligned} \quad (7)$$

In the second line above we used the notation

$$\eta_l = \text{sign } \text{d}U_l = \text{sign } \text{tr} U_{l_1}^\dagger U_{l_2} \quad (8)$$

and the change of variables $\sigma_l = A_l \eta_l$ to absorb the sign of $\text{d}U_l$ into a redefined gauge field on each link. The variables η_{C_i} and σ_{C_i} denote the product of η 's and σ 's around C_i .

The twisted partition sums $Z(\tau_1, \tau_2)$ can also be rewritten in the same fashion by absorbing the extra signs coming from the twist also in the σ 's choosing $\sigma_l = A_l \eta_l \tau_i$ on the twisted links. The only difference compared to (7) will be that the holonomies around C_1 and C_2 will pick up the twist τ_2 and τ_1 along the direction perpendicular to them. Accordingly the arguments of the corresponding delta functions will be multiplied by τ_1 for C_2 and τ_2 for C_1 . Contractible loops, in particular the boundaries of plaquettes always intersect the twists an even number of times therefore the plaquette delta functions do not have to be modified.

It is now easy to compute the order parameter $G(L)$ directly from its definition

$$\begin{aligned}
G(L) &= \frac{\int d\tau_1 d\tau_2 \tau_2 Z(\tau_1, \tau_2)}{\int d\tau_1 d\tau_2 Z(\tau_1, \tau_2)} \\
&= \frac{1}{Z} \prod_{s \in \Lambda} \int dU_s \prod_{l \in \Lambda} \int d\sigma_l \prod_{p \in \Lambda} \delta(d\sigma_p d\eta_p^{-1}) \sigma_{C_2} \eta_{C_2}^{-1} \exp\left(\beta \sum_{l \in \Lambda} \sigma_l |dU_l|\right), \quad (9)
\end{aligned}$$

where Z is exactly the same as the numerator of the r.h.s. except the factor $\sigma_{C_2} \eta_{C_2}^{-1}$ is missing. This factor in the numerator comes from the property of the delta function on $Z(2)$ that

$$\int d\tau \tau \delta(\tau \sigma) = \sigma. \quad (10)$$

The advantage of the normalisation that we chose for $G(L)$ is that in this way by integrating out the twist we could get rid of the delta functions constraining the holonomies around C_1 and C_2 in the “partition function” Z . This effectively means that we integrated out the $Z(2)$ part of the boundary conditions.

The remarkable property of this form of the partition function and $G(L)$ is that the integrand depends on the $SU(2)$ variables only through the $SU(2)/Z(2)$ cosets. In other words it has a $U_s \rightarrow -U_s$ local $Z(2)$ gauge symmetry and the spins can be regarded $SU(2)/Z(2) \equiv SO(3)$ variables rather than $SU(2)$ ones. Notice that the η_l 's themselves are not gauge invariant but products of them around any closed loop, in particular around plaquette boundaries and C_i are gauge invariant. The price that we pay for this extra gauge symmetry is the appearance of the new $Z(2)$ link variables σ_l .

3.2 $Z(2)$ strings and vortices

At this point it is in order to discuss the physical meaning of the degrees of freedom and excitations of the system that we obtained by rewriting the $SU(2)$ model in terms of $Z(2)$ and $SO(3)$ variables.

In (9) there are two different types of couplings between the $SO(3)$ spins U_s and the $Z(2)$ link variables σ_l . At first σ_l contributes an extra sign to the coupling between neighbouring $SO(3)$ spins residing on the two ends of the link l . If $\sigma_l = 1$ then these two spins are more likely to be parallel whereas for $\sigma_l = -1$ they tend to be “perpendicular”. In addition the plaquette delta functions constrain the “curvature” $d\sigma_p = \prod_{l \in \partial p} \sigma_l$ to be equal to $d\eta_p$.

The relevant $Z(2)$ excitations of the model are (stacks of) links with $\sigma_l = -1$, which we call σ -strings. These strings are either closed or they terminate on plaquettes having $d\sigma_p = -1$ i.e. an odd number of negative σ 's on their boundary. Due to the plaquette delta functions the end-plaquettes of σ -strings have to coincide with the $d\eta_p = -1$ plaquettes. For reasons that will become clear later we shall call these vortices.

In analogy with σ -strings we can also define η -strings as the location of $\eta_l = -1$ links. By construction every vortex is an endpoint of both a σ and an η -string (Fig 3). Notice however that the location of the η -strings does not have a physical meaning in terms of the $SO(3)$ variables, they can be deformed by $U_s \rightarrow -U_s$ gauge transformations. The location of vortices on the other hand is gauge invariant since $Z(2)$ gauge transformations always change the sign of an even number of factors in $d\eta_p$. The situation is analogous to gauge theories where one has Dirac strings attached to monopoles and the strings can be deformed by gauge transformations but their endpoints (boundaries in 4d), the monopoles (monopole loops) are gauge invariant objects.

It should be noted that there is a substantial difference between the energetics of the σ and η strings. To see this let us look at a closed contour of links enclosing exactly one vortex. Both the σ and the η string attached to the vortex have to pierce the contour somewhere. The link l where the σ string intersects the contour is unambiguously given by the $[\sigma]$ configuration and it carries an energy $\sim 2dU_l$. On the other hand as we have already seen, the location l' where the η string crosses the contour is not $Z(2)$ gauge invariant. It is thus not surprising that l' has no distinguished role among the links of the contour; it does not carry any extra energy. Indeed in a typical low temperature $SO(3)$ configuration the spins vary slowly around the contour and they make half of a complete turn as the contour encircles the vortex. This is more favourable both in terms of energy and entropy than having abrupt changes. Now we can see why the $d\eta_p = -1$ plaquettes were called vortices. $d\eta_p$ is well defined in terms of the $SO(3)$ variables and a "smooth" vortex configuration is a special case of defects appearing in 2d spin models due to the non simply-connectedness of the internal space [13].

At this point we want to emphasize that the internal space of the original $SU(2)$ spin model i.e. the $SU(2)$ group manifold is simply connected, therefore no vortices are present in the original model. After separating the $Z(2)$ degrees of freedom however, the remaining

(i.e. using a slowly varying “smooth” $\text{SO}(3)$ configuration) the energy of the η string can be easily seen to go as the log of its length. At low temperatures the vortices are in closely bound pairs due to the linearly confining potential of the σ string. Vortex pairs with short σ strings between them are local excitations, they are not expected to have a big influence on the large scale behaviour of the system. The η strings however can still fluctuate considerably because of their smaller energy cost and as we shall see long η strings are capable of disordering the system even on large distance scales.

At first sight one would expect that at sufficiently low temperature due to their logarithmic behaviour even the long η strings will freeze out of the system. This is however not quite right. To see this we have to notice that in the above semiclassical energy estimate we assumed that the lattice is very large compared to the length of the η string. Since we shall not be working directly in the infinite volume limit but rather consider the lattice size dependence of $G(L)$, this assumption may not be right. Indeed, let us look at two nearby vortices with a short σ string in between but the η string connecting them going all the way around the lattice. By a semiclassical argument similar to the one in Section 2.3 we can see that the energy of this configuration goes to a constant when $L \rightarrow \infty$. The two vortices of course can be removed by closing the η string around the lattice.

These types of configurations can potentially have a long range disordering effect. In fact it is exactly these configurations that have to be present with a sufficient weight to ensure that the relative difference between the twisted partition sum and the untwisted one decreases sufficiently rapidly with the lattice becoming larger. As we shall see later, this is what we need for $G(L)$ to decay exponentially.

3.3 Duality transformation

In the previous section we have succeeded in separating $\text{Z}(2)$ and $\text{SO}(3)$ variables in the $\text{SU}(2)$ spin model and showed that vortex and string excitations of the $\text{SO}(3)$ part can have a long range disordering effect. Unfortunately the $\text{Z}(2)$ part of the system does not look very familiar and in order to proceed we want to cast it into a more manageable form. This can be done by a duality transformation on the σ link variables which amounts to trading them for $\text{Z}(2)$ plaquette variables that we call ω_p . The interaction between ω 's will turn out to

be nearest neighbour ferromagnetic although with fluctuating couplings that depend on the SO(3) spin configuration. The ω 's in this way give an Ising model on the dual lattice the sites of which are plaquettes of the original lattice.

Technically the Z(2) duality transformation is done by expanding each factor in the integrand of $G(L)$ (equation (9)) depending on the σ 's in terms of Z(2) characters as

$$f(\sigma) = \hat{f}(1) + \sigma \hat{f}(-1) = \int d\alpha \hat{f}(\alpha) \chi_\alpha(\sigma). \quad (11)$$

The expansion for the different factors in (9) reads as

$$\begin{aligned} \delta(d\sigma_p d\eta_p^{-1}) &= \int d\omega_p \chi_{\omega_p}(d\sigma_p d\eta_p^{-1}) \\ \sigma_{C_2} &= \chi_{-1}(\sigma_{C_2}) = \prod_{l \in C_2} \chi_{-1}(\sigma_l) \\ e^{\sigma_l |dU_l|} &= \int d\alpha_l \chi_{\alpha_l}(\sigma_l) e^{\mathcal{L}(dU_l, \alpha_l)}, \end{aligned} \quad (12)$$

where $e^{\mathcal{L}(dU_l, \alpha_l)}$ is the Z(2) ‘‘Fourier transform’’ of $e^{\sigma_l |dU_l|}$ and for later convenience it can be split into a part depending only on the SO(3) variables and another one depending both on the SO(3) and Z(2) degrees of freedom;

$$e^{\mathcal{L}(dU_l, \alpha_l)} = \frac{1}{2} \left(e^{\beta |dU_l|} + \alpha_l e^{-\beta |dU_l|} \right) = e^{M(dU_l)} e^{\alpha_l K(dU_l)}. \quad (13)$$

Here the functions K and M are given by

$$M(dU_l) = \frac{1}{2} \ln \sinh(2\beta |dU_l|) \quad \text{and} \quad K(dU_l) = \frac{1}{2} \ln \coth(\beta |dU_l|). \quad (14)$$

Substituting these into the expression (9) of $G(L)$ the σ variables can be explicitly integrated out using the orthogonality of the characters. This will give rise to constraints between the remaining Z(2) degrees of freedom, namely on each link

$$\alpha_l = d^* \omega_l = \prod_{p: l \in \partial p} \omega_p \quad (15)$$

except on the links belonging to C_2 where $\alpha_l = -d^* \omega_l$. These constraints make the α_l integrals trivial and yield

$$\begin{aligned} G(L) &= \frac{1}{Z} \int d\nu[U] \prod_{p \in \Lambda} \int d\omega_p \chi_{\omega_p}(d\eta_p) \\ &\quad \times \eta_{C_2} \exp \left(\sum_{l \notin C_2} K(dU_l) d^* \omega_l - \sum_{l \in C_2} K(dU_l) d^* \omega_l \right), \end{aligned} \quad (16)$$

where

$$d\nu[U] = \prod_{s \in \Lambda} dU_s e^{\beta \sum_l M(dU_l)} \quad (17)$$

is the SO(3) (Z(2) gauge invariant) part of the measure.

Exactly the same transformation can be carried out on the partition function Z , the only difference in the final result compared to (16) will be the absence of the factor η_{C_2} and the minus sign in the couplings between ω 's along C_2 .

In this representation the system consists of Z(2) spins ω_p attached to plaquettes and the SO(3) part of the system is unchanged. The ω 's on nearest neighbour plaquettes sharing the link l interact via the coupling $K(dU_l)$. The Z(2) part of the system is essentially an Ising model on the dual lattice although the spin-spin couplings can fluctuate since they depend on the SO(3) configuration.

For large β the effective SO(3) action $M(dU_l)$ is peaked at the maximum of $|dU_l|$ which means that $\beta|dU_l|$ is also large for “most” of the relevant configurations. The asymptotic behaviour of $M(dU_l)$ in this limit is $\sim \beta|dU_l| - \ln 2/2$. On the other hand the duality transformation changes low temperature to high temperature for the Z(2) part of the system. Indeed the $\beta \rightarrow \infty$ limit of the effective Ising coupling is $K(dU_l) \sim e^{-2\beta|dU_l|}$.

4 Construction of the effective Ising model

We have seen that after separating the Z(2) and SO(3) variables in the SU(2) model, $G(L)$ can be rewritten in terms of a dual Ising model coupled to SO(3) spins. As can be seen from equation (16) the Ising part of $G(L)$ is essentially the ratio between a twisted (along C_2) and the untwisted partition sum, i.e. the free energy of a twist along C_2 ($G^*(L)$ in the language of Section 2). Notice that because of the duality transformation, $G(L)$ in the original model is becomes $G^*(L)$ in the dual Ising model.

We have already discussed that the Ising couplings between nearest neighbour plaquettes depend on the SO(3) spin configuration. Besides there are two more SO(3) dependent pieces in the expression of $G(L)$; η_{C_2} and the product of group characters $\chi_{\omega_p}(d\eta_p)$. While η_{C_2} depends solely on the SO(3) variables, the group characters couple vortices to the Ising spins on each plaquette.

For a fixed $\text{SO}(3)$ configuration with vortices at $(p_1, p_2 \dots p_{2n})$ and S η strings⁵ crossing C_2 these give an overall factor of $(-1)^S \prod_{i=1}^{2n} \omega_{p_i}$. Were it not for this additional factor depending on the $\text{SO}(3)$ configuration, the $\text{Z}(2)$ part of the system would be a ferromagnetic Ising model at high temperature with unbroken symmetry and $G(L)$, the ratio of the twisted and untwisted partition sum would go to a nonzero constant on large lattices. It follows that if we were to eliminate all the vortices from the measure and also constrain η_{C_2} to be +1 the exponentially falling asymptotic behaviour of $G(L)$ would be lost. The configurations responsible for the correct asymptotic behaviour of $G(L)$ are exactly those that would be eliminated by the above constraints.

4.1 Strings and vortices in the dual representation

Let us now have a closer look at the relevant configurations in the different vortex sectors. In the absence of vortices the only difference between the numerator and the denominator of (16) is the factor η_{C_2} . This is true up to graphs of size $\sim L$ in the high temperature expansion of the ω Ising model but these are exponentially suppressed (see Section 2.2). All the short contractible η strings have to cross C_2 an even number of times and they do not contribute to η_{C_2} . $\eta_{C_2} = -1$ thus means that there is an odd number of η strings winding around the lattice perpendicularly to C_2 . In the zero-vortex sector it is exactly the long topologically nontrivial η strings that give a negative contribution to the numerator of $G(L)$ and a positive one to the denominator. If there were no vortices at all, the asymptotic behaviour of $G(L)$ would solely depend on the relative weight of these configurations.

Let us now consider the sector with two nearby vortices at p_1 and p_2 . In this sector the high-temperature expansion of the ω spin system contains small graphs connecting p_1 and p_2 . If a graph like this crosses C_2 then in the numerator it acquires a minus sign due to the twist. Besides we still have the factor η_{C_2} . The combined effect of these two signs will be different for the numerator and the denominator of (16) only if the ω graph together with the η string connecting the two vortices close into a noncontractible loop (Fig 4). This is absolutely essential, otherwise the sign coming from η_{C_2} would cancel the one coming from

⁵Although S is not well defined in terms of the $\text{SO}(3)$ variables, its parity $(-1)^S$ is invariant under coset reparametrisations

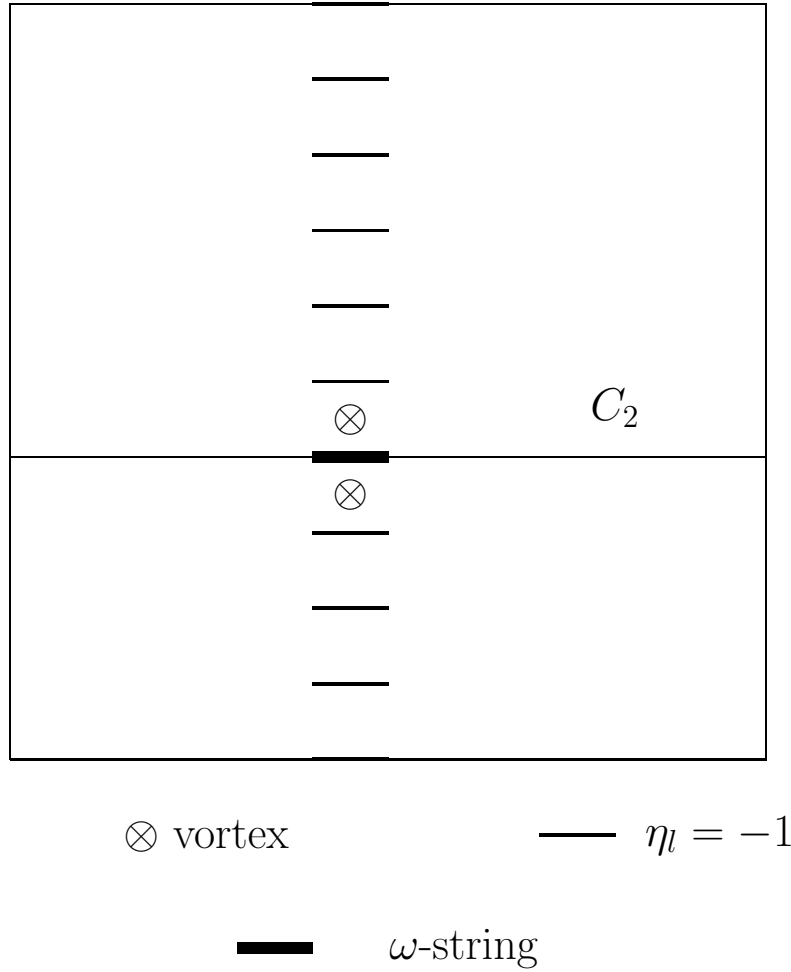


Figure 4: A vortex pair with its connecting η and ω string forming a noncontractible loop winding around the lattice. This configuration gives different contributions to the numerator and denominator of $G(L)$.

the twist. In other words the curve C_2 could be deformed by a $Z(2)$ gauge transformation to decouple from both the ω and the η string (as in Fig 5). This obviously cannot be done with the configuration in Fig 4.

The configuration in Fig 4 is not very much different from the one discussed in the 0-vortex sector. Again it contains a long η string winding almost around the lattice connecting the two vortices with a small gap between them.

We can already see the similarity between this expansion and the high temperature expansion of the Ising model with a nonzero magnetic field discussed in Section 2.2. The

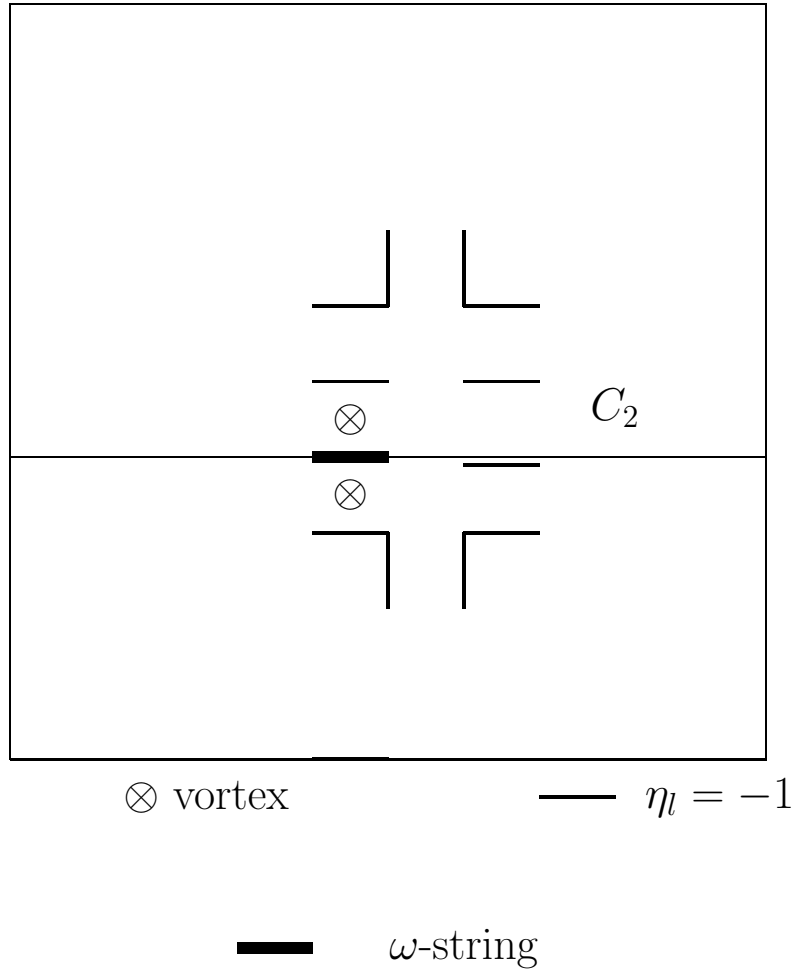


Figure 5: A vortex pair with the connecting η and ω string forming a contractible loop. This graph gives the same contribution to the numerator and the denominator of $G(L)$.

only difference here is that the graphs of order $2n$ are proportional to $2n$ -vortex expectations instead of the $2n$ -th power of the magnetic field. It should be stressed that the vortex expectations have to be calculated with the $SO(3)$ measure (17) which is “blind” to the centre of $SU(2)$.

The similarity between the two expansions hints that it might be possible to approximate the dual representation of the $SU(2)$ model with an effective Ising model. In this way we could trade the $SO(3)$ variables for a suitably chosen effective coupling $K_{\text{eff}}(\beta)$ and an effective magnetic field $h(\beta)$. To put it more precisely, we want to bound expression (16) of $G(L)$ by the ratio of the twisted and untwisted partition function of an Ising model with a suitably

chosen coupling $K_{\text{eff}}(\beta)$ and a magnetic field $h(\beta)$. For large β K_{eff} and h will be exponentially small and the high temperature expansion for the effective Ising model will be convergent. As we saw in Section 2.2 in the presence of a nonzero magnetic field the ratio of the twisted partition function to the untwisted one falls off exponentially with the lattice size. It means that if the Ising bound for $G(L)$ can be established with a *nonzero* magnetic field it would imply the exponential decay of $G(L)$.

To summarize, in order to explicitly construct the effective Ising model we have to deal with three questions.

- The fluctuating couplings $K(dU_l)$ have to be approximated by some K_{eff} .
- The effect of the $\text{SO}(3)$ vortices on the Ising spins has to be substituted with an external magnetic field.
- Somehow we have to get rid of the factor η_{C_2} that depends only on the $\text{SO}(3)$ variables.

The last point turns out to be the simplest one. Since long η strings disorder the system, constraining η_{C_2} to be $+1$ makes the system more ordered and increases $G(L)$. Indeed by using reflection positivity it can be proved that this constraint increases $G(L)$ [12]. From this point on we shall consider the quantity $G(L, C_2^+)$ which is defined as $G(L)$ calculated with this additional constraint. The $\text{SO}(3)$ measure $d\nu[U]$ supplemented with this constraint will be called $d\nu_+[U]$.

4.2 The effective Ising coupling

We now want to compare $G(L, C_2^+)$ with the quantity

$$G_{\text{eff}}(h, K_{\text{eff}}, L) = \frac{1}{Z_{\text{eff}}} \prod_{s \in \Lambda} \int d\omega_p \exp \left(K_{\text{eff}} \sum_{l \notin C_2} d^* \omega_l - K_{\text{eff}} \sum_{l \in C_2} d^* \omega_l + h \sum_{p \in \Lambda} \omega_p \right), \quad (18)$$

i.e. the ratio of the twisted and untwisted partition function of an Ising model.

In the original $\text{SU}(2)$ model we started with the particular form of the interaction $dU_l = \text{tr} U_{1l}^\dagger U_{2l}$. We could have as well used any other action in the same universality class. In particular the choice

$$S = \sum_{l \in \Lambda} |dU_l| + \mu \sum_{l \in \Lambda} \eta_l \quad (19)$$

with $\mu > 0$ would have considerably simplified the discussion. After the separation of the $Z(2)$ variables and the duality transformation on this action we get

$$M(dU_l) = \beta |dU_l| \quad \text{and} \quad K(dU_l) = \frac{1}{2} \ln \coth 2\mu\beta, \quad (20)$$

i.e. the Ising coupling is independent of the $SO(3)$ variables and we do not need to find an approximation for K_{eff} . Because of its simplicity we shall only consider this form of the action and the quantity $G(C_2^+, \mu, L)$ corresponding to $G(L, C_2^+)$ with this particular choice of the $SU(2)$ action.

4.3 Ginibre decomposition

We now want to find a nonzero magnetic field h , independent of the lattice size such that on any lattice

$$G_{\text{eff}}(h, K, L) - G(C_2^+, \mu, L) \geq 0. \quad (21)$$

This would imply the exponential fall-off of $G(C_2^+, \mu, L)$ and by the inequalities proved so far the same behaviour for the correlation function of the $SU(2)$ spin model.

By an argument similar to Ginibre's proof of the Griffiths' inequalities [14] the difference $Z_{\text{eff}}Z(G_{\text{eff}} - G)$ can be decomposed into a sum of terms independent of the ω variables, containing only vortex correlations calculated with the $SO(3)$ measure $d\nu_+[U]$, including the constraint on the η string. Details of this decomposition can be found in the Appendix. The form of these terms is (up to non-negative constant factors)

$$D(\hat{h}) = \left\langle \prod_{p \in \bar{\Lambda}} (\theta_p^- \pm \hat{h}\theta_p^+) \prod_{p \notin \bar{\Lambda}} (\theta_p^+ \pm \hat{h}\theta_p^-) \right\rangle_L, \quad (22)$$

where $\langle \rangle_L$ means expectation with respect to the $SO(3)$ measure $d\nu_+[U]$, $\bar{\Lambda}$ is some subset of Λ containing an even number of plaquettes and $\hat{h} = \tanh h$.

It is easily seen that for $\hat{h} = 0$ all these diagrams are strictly positive implying that $G_{\text{eff}}(h = 0, K, L) > G(C_2^+, \mu, L)$. On any finite lattice G_{eff} is an analytic function of h and this inequality is in fact true not only for $h = 0$ but for any h in some finite interval around 0. However we still need to establish that this interval does not shrink to zero as the lattice size goes to infinity.

5 Vortex correlations

In this section we want to study the dependence of the vortex expectations (22) on the effective magnetic field and make it plausible that there is a finite interval around $h = 0$ for which all these expectations are non-negative independently of the lattice size. We would like to emphasize that up to this point all our arguments were rigorous.

5.1 Factorisation inequality

Vortex expectations of the type (22) come in huge varieties. We can introduce some order into this abundance by explicitly constraining out some of the $Z(2)$ excitations while still keeping a finite density of them. This will certainly make the system more ordered and the presence of a mass gap in this system would imply a mass gap in the original model. With these further constraints we can essentially pair up vortices so that the remaining nonzero expectations of the type (22) will have the form

$$D(\hat{h}) = \left\langle \prod_{P_i \in \tilde{\Lambda}} (\theta_{P_i}^- - \hat{h} \theta_{P_i}^+) \prod_{p \notin \tilde{\Lambda}} \theta_p^+ \right\rangle, \quad (23)$$

where $\tilde{\Lambda}$ is a sublattice of Λ , $P_i = \{p_{i1} p_{i2}\}$ denotes pairs of plaquettes and $\theta_{P_i}^\pm = \theta_{p_{i1}}^\pm \theta_{p_{i2}}^\pm$.

Now for $\hat{h} = 0$ it can be proved that

$$\left\langle \prod_{P_i \in \tilde{\Lambda}} \theta_{P_i}^- \prod_{p \notin \tilde{\Lambda}} \theta_p^+ \right\rangle \geq \prod_{i=1}^n \left\langle \theta_{P_i}^- \prod_{p \notin P_i} \theta_p^+ \right\rangle. \quad (24)$$

This correlation inequality can be checked by using reflection positivity for vortex configurations that are symmetrically placed about a line bisecting the lattice. For more general configurations the proof involves the application of the FKG inequalities [15].

Now it is quite plausible that if the above factorisation inequality holds for $\hat{h} = 0$ then it will be true for some finite interval around $\hat{h} = 0$ which is independent of the lattice size. Let us for the moment assume this. It follows then that we have a lower bound on $G_{\text{eff}} - G$ in terms of a sum that contains products of two-vortex expectations of the form

$$\prod_{i=1}^n \left\langle (\theta_{P_i}^- - \hat{h}^2 \theta_{P_i}^+) \prod_{p \notin P_i} \theta_p^+ \right\rangle \quad (25)$$

It is now enough to establish that all these factors are non-negative for any \hat{h} in some finite interval around zero independent of the lattice size. This is equivalent to the statement that the free energy of a vortex pair (as compared to that of the no-vortex state),

$$F_L(p_1, p_2) = -\frac{1}{\beta} \frac{\langle \theta_{p_1}^- \theta_{p_2}^- \prod_{p \neq p_1, p_2} \theta_p^+ \rangle}{\langle \prod_{p \in \Lambda} \theta_p^+ \rangle}, \quad (26)$$

is bounded for arbitrarily large lattices. Normally one would think about a pair of vortices as a local excitation and its free energy is not expected to diverge with the lattice size. This is however not trivially true in our case due to the constraint on the η string contained in the measure $d\nu_+[U]$. If the two nearby vortices are cut off from each other by C_2 , their connecting η string has to wind around the lattice to avoid crossing C_2 . This type of excitation is definitely not a local object. In fact the “most non-local” excitation in the two-vortex sector is the one that has two adjacent vortices separated by C_2 (see Figure 4). All other types of two-vortex configurations contain shorter η strings and therefore have a smaller free energy.

In two dimensions, as we have already seen, the free energy of such a long η string stays finite as $L \rightarrow \infty$ in the semiclassical approximation. This is due to flux spreading that allows the cost of the string creation to spread laterally in the direction perpendicular to the string. Intuitively one expects the spreading of the flux to be even faster than that given by the semiclassical approximation but unfortunately we could not prove this analytically. Instead we measured the lattice size dependence of the two-vortex free energy using Monte Carlo.

5.2 Monte Carlo results

In this subsection we want to give some evidence that the free energy of two adjacent vortices separated by the curve C_2 does not diverge when the lattice size goes to infinity. Moreover we claim that this is very likely to be true for any non-zero temperature.

It is well-known that both in non-Abelian 2D spin models and the analogous 4D gauge theories the strong and weak coupling regions are separated by a crossover region, where the specific heat has a finite peak [16]. We used the specific heat peak to ensure that the coupling that we use in the simulations is already “weak”. The Monte Carlo simulation was performed at $\beta = 2.0$ which is already in the weak coupling region as can be seen from

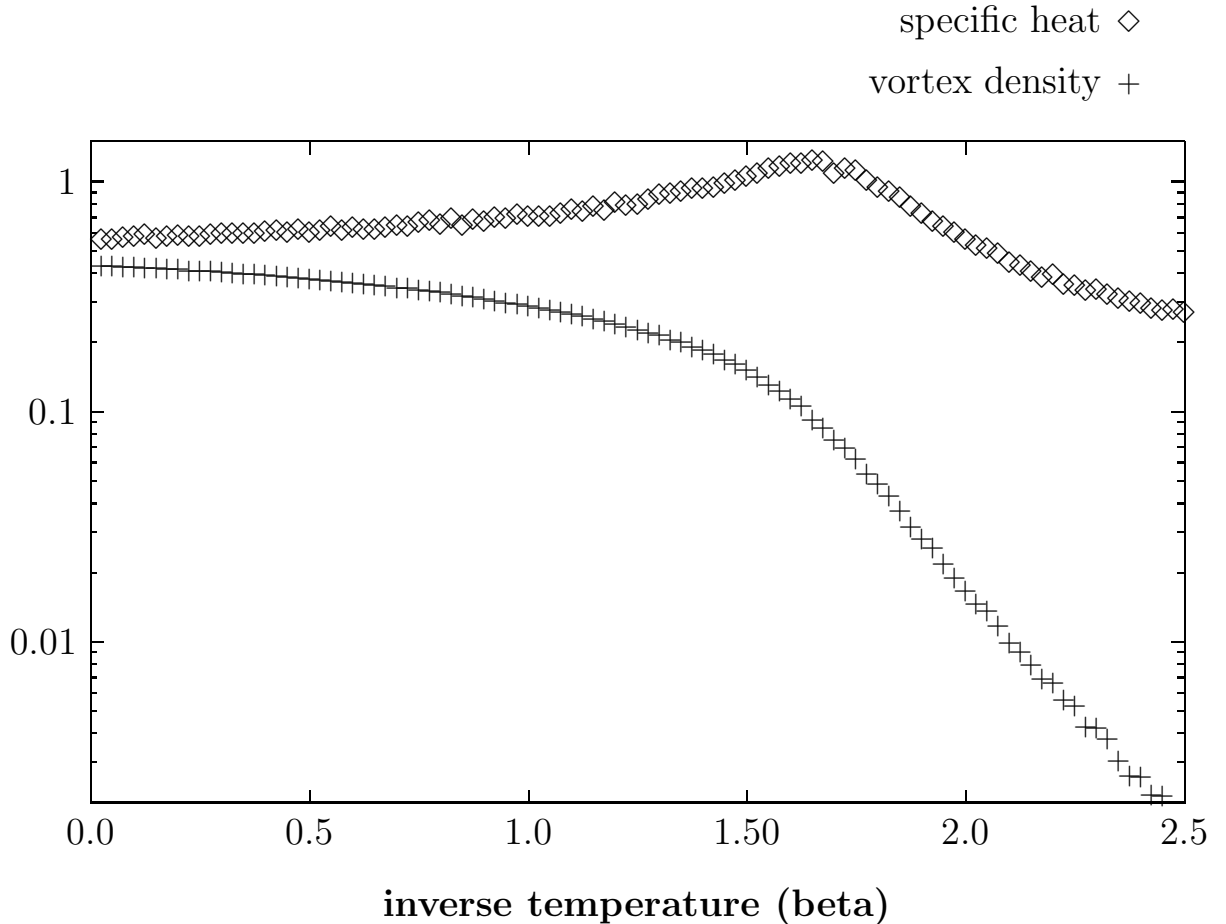


Figure 6: The specific heat and the vortex density versus inverse temperature (β) on an 8×8 lattice calculated with the $SO(3)$ action.

Figure 6. We also plotted in the same Figure the $Z(2)$ vortex density versus the inverse temperature. Another characteristic feature of the weak coupling region is that the vortex density (monopole density in gauge theories) decreases exponentially as a function of β [16]. This can also be clearly seen in the Figure.

We do not expect any dramatic phenomenon to happen when going from the weak coupling side of the specific heat peak to even weaker and weaker couplings, therefore our results should qualitatively apply for any “weak” but of course non-zero coupling.

We measured the probability of the configuration with two adjacent vortices at fixed positions separated by C_2 , normalised by the probability of having no vortices at all. The calculation was done by generating a series of configurations using a local heat bath algorithm

with the $\text{SO}(3)$ invariant measure $d\nu[U]$ but *without the constraint on the η string*. In a long Monte Carlo run the number of configurations of the type in Figure 4 was counted and divided by the number of configurations with no vortices at all and an even number of η strings crossing C_2 .

Since (at fixed β) on larger lattices there are typically more vortices, the probability of the configurations with exactly zero and one vortex pair decreased very rapidly with increasing lattice size. This meant that the quantity we wanted to measure was given as a ratio between two numbers both becoming very small on larger lattices, however their ratio was expected to be stable. This made the signal less accurate on larger lattices. An improvement by a factor L^2 could be achieved by counting all the configurations that were translations of the one in Figure 4 and dividing the result by L^2 . Because of the periodic boundary conditions the lattice had an exact translation invariance and this procedure did not change the results.

The simulations were performed on square lattices of $5 \leq L \leq 13$. The rapidly deteriorating quality of the signal made it impossible to go beyond $L = 13$. Even at this point we typically needed several hundred thousands of independent configurations to get a signal at all. Our results are summarised in Figure 7. We can see that the probability of a vortex pair with a long η string decreases on small lattices until it stabilises at a moderate lattice size ($L \approx 8 - 9$) and stays constant thereafter. Recall that for our purposes it is enough if this quantity remains non-zero in the $L \rightarrow \infty$ limit.

To study the spreading of the flux of the long eta string, we measured the same quantity with the lattice size fixed in the direction parallel to the string and varied in the perpendicular direction. The results are plotted in Figure 8. The pronounced effect of flux spreading is obvious; as the lattice becomes wider, there is more space available for the flux of the η string to spread and its probability increases dramatically.

To summarise, our Monte Carlo results are qualitatively consistent with the semiclassical picture of flux spreading and it is indeed very hard to imagine that anything could happen either at higher β or larger lattice sizes that could make the two-vortex probability vanish in the $L \rightarrow \infty$ limit. Of course our results do not imply any particular analytic form as to how the flux actually spreads and it seems very hard to distinguish between a semiclassical “massless” spreading and an exponential spreading. This is however not necessary for our purposes; the only property that we need is that the probability of the long string with two

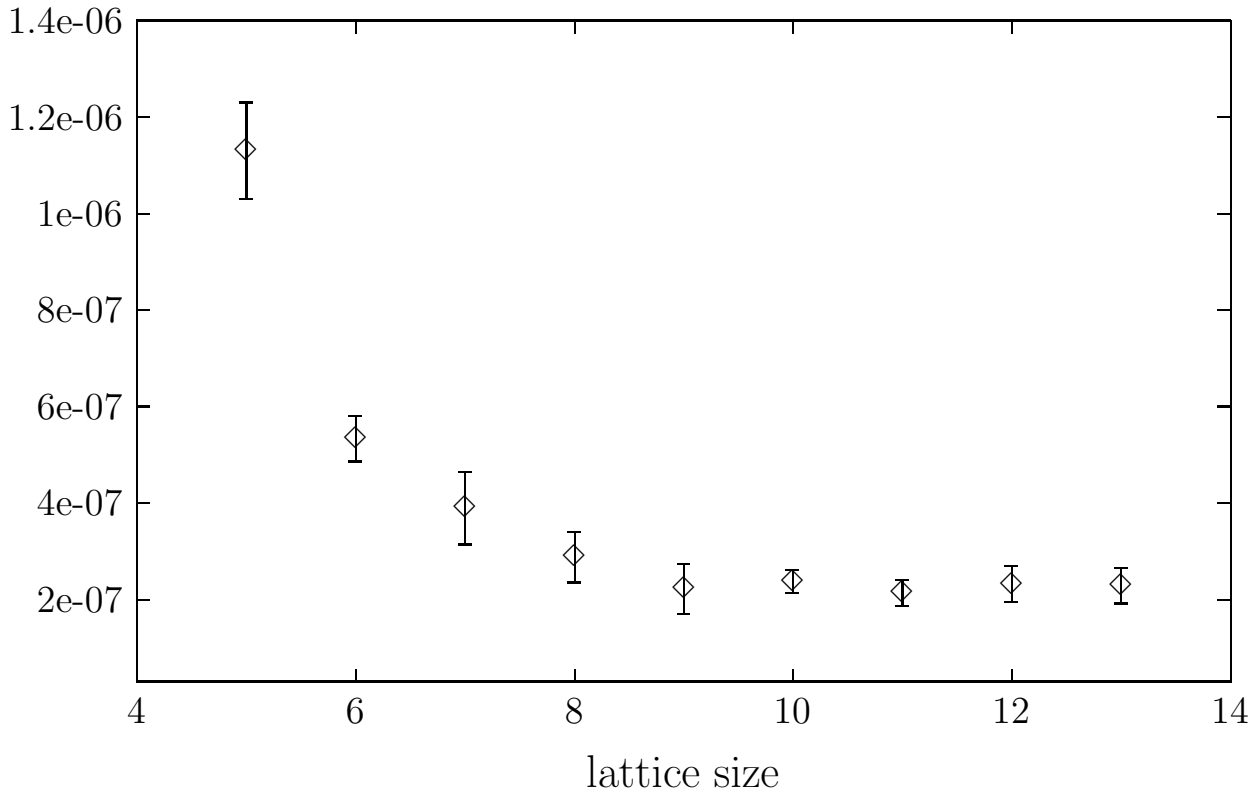


Figure 7: The probability of a neighbouring vortex pair with its η string winding around the lattice (see Fig 4) as a function of the lattice size at $\beta = 2.0$. The measurement was done with the SO(3) action.

vortices remain non-zero in the $L \rightarrow \infty$ limit.

6 Conclusions

We proposed a mechanism that is sufficient to create a nonzero mass gap in the SU(2) chiral spin model at arbitrarily small temperatures. Instead of considering the correlation function we were looking at an operator ($G(L)$, the twist) that measured how effective fluctuations were in destroying the correlations between the “relative signs” of spins at different locations.

In this way we could separate the spin system into two interacting parts, a Z(2) and an SO(3). We derived the conditions that the SO(3) part had to satisfy so that the mass gap

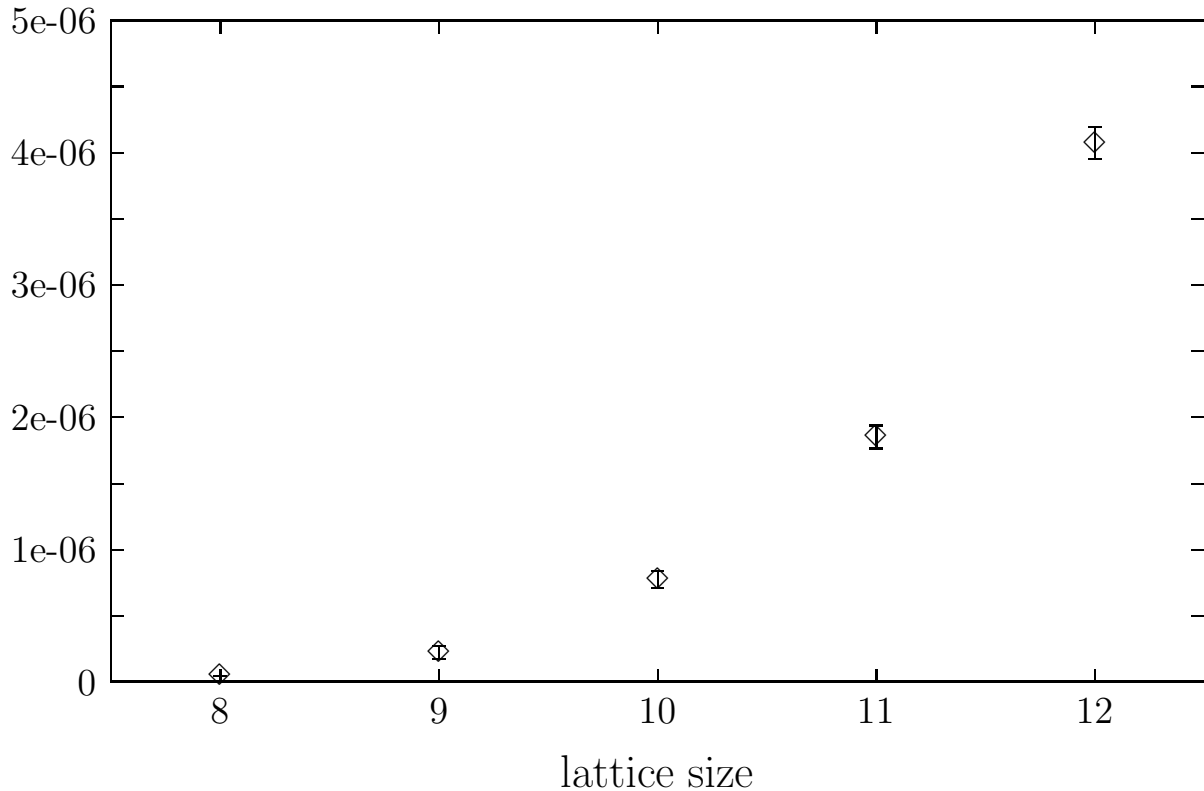


Figure 8: The same as in Figure 7 except that instead of using a square lattice the length in the direction parallel to the η string was fixed to 9 and only the transverse (perpendicular to the string) size was varied.

could be rigorously established in terms of an effective $Z(2)$ system, which was an Ising model on the dual lattice. By using a plausible (but so far not proved) vortex correlation inequality we could reduce these necessary conditions to just one condition, namely the boundedness of the free energy of a vortex pair connected by an η string winding around the lattice for any lattice size.

This condition on the truly non-Abelian part of the system was substantially weaker than the existence of a mass gap itself. The presence of a mass gap would require that an external $Z(2)$ flux, introduced by twisted boundary conditions, spread exponentially fast on large lattices, i.e. the expectation of a twist would have to go to 1 exponentially. On the other hand in our scheme we only needed that the expectation of the twist be non-zero for

asymptotically large lattices. It is nevertheless surprising that we failed to verify even this substantially weaker condition rigorously and eventually we had to resort to Monte Carlo to check it. As expected, our Monte Carlo data show that even at low temperature the expectation of the twist goes to a nonzero constant as $L \rightarrow \infty$. It would be however very desirable to have an analytic proof of this and the vortex correlation inequalities too.

This framework can also be applied to 3d and 4d $SU(2)$ gauge theories with essentially no modifications. The only minor difference here is that the corresponding objects on the lattice live on higher dimensional simplices. For example instead of $Z(2)$ vortices on plaquettes we have $Z(2)$ monopoles (monopole loops in 4d) on cubes and the twist in the spin model is exactly analogous to the sourceless 't Hooft loop in gauge theories (for a definition see [8]). In this way the confinement problem can be reduced to $Z(2)$ monopole correlation inequalities. Monte Carlo results concerning the relevant monopole correlations will be reported elsewhere [17]. This gives a unifying picture of confinement in gauge theories and disorder in spin models.

To summarise, we rigorously proved that the presence of a mass gap in the 2d $SU(2)$ chiral spin model at low temperature is tantamount to certain vortex correlation inequalities in a related $SO(3)$ spin model. These inequalities in turn have been (partly) checked by Monte Carlo calculations. It would be worthwhile to obtain an analytic proof of the vortex correlation inequalities and thus complete the solution of this longstanding problem. Finally, it would be also interesting to extend this scheme to other symmetry groups, in particular to $SU(n)$.

Acknowledgement

I am grateful to Terry Tomboulis for introducing me to this problem and also for many helpful conversations. I also thank the Department of Theoretical Physics, Kossuth University, Debrecen, Hungary for granting me part of the computer time used for the Monte Carlo.

References

- [1] Fröhlich, J. and Spencer, T., Commun. Math. Phys. **81** (1981) 527

- [2] Hasenfratz, P., Maggiore, M. and Niedermayer, F., Phys. Lett. **B245** (1990) 522; Hasenfratz, P. and Niedermayer, F., Phys. Lett. **B245** (1990) 529; Balog, J., Naik, S., Niedermayer, F. and Weisz, P., Phys. Rev. Lett. **69** (1992) 873; Hollowood, T.J., Phys. Lett. **B329** (1994) 450
- [3] Campostrini, M., Rossi, P. and Vicari, E., Phys. Rev. **D52** (1995) 386
- [4] Guth, A.H., Phys. Rev. **D21** (1980) 2291
- [5] Tomboulis, E.T., Phys. Lett. **B303** (1993) 103; Nucl. Phys. B Proc. Suppl. **30** (1993) 549; Nucl. Phys. B Proc. Suppl. **34** (1994) 192
- [6] Kovács, T.G. and Tomboulis, E.T., Phys. Lett. **B321** (1994) 75
- [7] Kovács, T.G. and Tomboulis, E.T., Phys. Lett. **B367** (1996) 254
- [8] Tomboulis, E.T. and Yaffe, L.G., Commun. Math. Phys. **100** (1985) 313
- [9] Groeneveld, J., Jurkiewicz, J. and Korthals Altes, C.P., Physica Scripta **23** (1981) 1022
- [10] 't Hooft, G., Nucl. Phys. **B153** (1979) 141
- [11] Yaffe, L.G., Phys. Rev. **D21** (1979) 1574
- [12] Kovács, T.G., UCLA Ph.D. Thesis, in preparation
- [13] Mermin, N.D., Rev. Mod. Phys. **51** (1979) 591
- [14] Ginibre, J., Commun. Math. Phys. **16** (1970) 310
- [15] Fortuin, C.M., Kasteleyn, P.W. and Ginibre, J., Commun. Math. Phys. **22** (1971) 89
- [16] Kogut, J., Snow, M. and Stone, M., Nucl. Phys. **B215** (1983) 45; Sinclair, D.K., Nucl. Phys. **B205**[FS5] (1982) 173; Brower, R.C., Kessler, D.A. and Levine H., Nucl. Phys. **B205**[FS5] (1982) 77; Caneschi, L., Halliday, I.G. and Schwimmer, A., Nucl. Phys. **B200**[FS4] (1982) 409
- [17] T.G. Kovács and E.T. Tomboulis, in preparation

Appendix

In the Appendix we derive the decomposition of $Z_{\text{eff}}Z(G_{\text{eff}} - G)$ into a sum of vortex expectations with non-negative coefficients. Using (18) and (16) (with the measure $d\nu_+[U]$ and $K(dU_l)$ computed from (20)) this can be written as a double Z(2) integral for two independent copies of the ω variables on each plaquette,

$$Z Z_{\text{eff}}(G_{\text{eff}} - G) = \int d\nu_+[U] \prod_{p \in \Lambda} \int d\omega_p \int d\tilde{\omega}_p \chi_{\omega_p}(d\eta_p) e^{h\tilde{\omega}_p} \exp \sum_{l \notin C_2} K(d^*\omega_l + d^*\tilde{\omega}_l) \\ \times \left[\exp \sum_{l \in C_2} K(d^*\omega_l - d^*\tilde{\omega}_l) - \exp - \sum_{l \in C_2} K(d^*\omega_l - d^*\tilde{\omega}_l) \right]. \quad (27)$$

We shall make use of the identity

$$\prod_{i=1}^n f_i - \prod_{i=1}^n g_i = \frac{1}{2^{n-1}} \sum_{\{+-\dots\}} \prod_{i=1}^n (f_i \pm g_i), \quad (28)$$

where the summation is on all possible strings of plus and minus signs of length n containing an odd number of minus signs. This can be easily verified by induction on n (see [14]).

Now by applying this identity on the expression in the second line of (27) it can be written as

$$\exp K \sum_{l \in C_2} (d^*\omega_l - d^*\tilde{\omega}_l) - \exp -K \sum_{l \in C_2} (d^*\omega_l - d^*\tilde{\omega}_l) = \\ \frac{1}{2^{L-1}} \sum_{\{+-\dots\}} \prod_{l \in C_2} \left[e^{K(d^*\omega_l - d^*\tilde{\omega}_l)} \pm e^{-K(d^*\omega_l - d^*\tilde{\omega}_l)} \right]. \quad (29)$$

We can now expand all the factors in the integrand of (27) using

$$f(\omega) = \hat{f}(1) \left(1 + \omega \frac{\hat{f}(-1)}{\hat{f}(1)} \right), \quad (30)$$

(see equation (11)) and then make a change of variables

$$\omega^+ = \frac{1}{2}(\omega + \tilde{\omega}) \quad \text{and} \quad \omega^- = \frac{1}{2}(\omega - \tilde{\omega}) \quad (31)$$

on each plaquette. This will result in an expression containing factors of the form $(\omega^+)^{n_p}(\omega^-)^{m_p}$ on each plaquette and the rest of the integrand will be independent of the ω 's. Upon integrating out the ω 's and $\tilde{\omega}$'s each plaquette contributes a factor

$$\int d\omega_p \int d\tilde{\omega}_p (\omega_p^+)^{n_p} (\omega_p^-)^{m_p} = \frac{1}{2} \delta_{n_p,0} \delta_{m_p,\text{even}} + \frac{1}{2} \delta_{m_p,0} \delta_{n_p,\text{even}}, \quad (32)$$

where $\delta_{n_p \text{ even}} = 1$ if n is even, 0 otherwise. This means that each plaquette can have only an even power of one type of ω (+ or -) otherwise the corresponding term vanishes.

In the following we list the expansion of different factors in the integrand of (27) in terms of the ω^\pm 's. Since we want to verify only the positivity of each term in the expansion of (27) we shall sometimes omit positive constant factors and in these cases use “ \approx ” instead of “ $=$ ”.

The plaquette factors can be written as

$$\chi_{\omega_p}(\text{d}\eta_p) e^{h\tilde{\omega}_p} = (\theta^+ + \theta^- \omega_p)(\cosh h + \tilde{\omega}_p \sinh h) \approx (\theta^+ + \theta^- \omega_p)(1 + \tilde{\omega}_p \hat{h}), \quad (33)$$

where θ_p^\pm are projection operators onto states without/with (+/-) a vortex at p , $\hat{h} = \tanh h$ and we have omitted the trivial constant factor $\cosh h$. After the change of variables (31) this becomes

$$\begin{aligned} \chi_{\omega_p}(\text{d}\eta_p) e^{h\tilde{\omega}_p} &= (\theta_p^- + \hat{h}\theta_p^+) \omega_p^+ + (\theta_p^- - \hat{h}\theta_p^+) \omega_p^- + \\ &\quad \frac{1}{2}(\theta_p^+ + \hat{h}\theta_p^-) (\omega_p^+)^2 + \frac{1}{2}(\theta_p^+ - \hat{h}\theta_p^-) (\omega_p^-)^2 \end{aligned} \quad (34)$$

The links not belonging to C_2 can be expanded as

$$\begin{aligned} e^{K\text{d}^*\omega_l + K\text{d}^*\tilde{\omega}_l} &\approx (1 + \hat{K}\text{d}^*\omega_l)(1 + \hat{K}\text{d}^*\tilde{\omega}_l) = \\ &\hat{K}(\text{d}^*\omega_l + \text{d}^*\tilde{\omega}_l) + \frac{1 + \hat{K}^2}{4}(\text{d}^*\omega_l + \text{d}^*\tilde{\omega}_l)^2 + \frac{1 - \hat{K}^2}{4}(\text{d}^*\omega_l - \text{d}^*\tilde{\omega}_l)^2 \end{aligned} \quad (35)$$

To rewrite this in terms of ω_{l1}^\pm and ω_{l2}^\pm , the ω^\pm variables on the two plaquettes sharing the link l , we can apply the following identities that can be easily checked by using the definition of the ω^\pm 's;

$$\omega_1 \omega_2 \pm \tilde{\omega}_1 \tilde{\omega}_2 = 2(\omega_1^+ \omega_2^\pm + \omega_1^- \omega_2^\mp) \quad (36)$$

$$(\omega_1 \omega_2 \pm \tilde{\omega}_1 \tilde{\omega}_2)^2 = 4 \left[(\omega_1^+)^2 (\omega_2^\pm)^2 + (\omega_1^-)^2 (\omega_2^\mp)^2 \right] + \dots \quad (37)$$

The ellipses in the second identity means that terms that integrate to zero because they contain both ω^+ and ω^- on the same plaquette have been omitted. Now the final form of the expansion for links not contained in C_2 is

$$\begin{aligned} e^{K\text{d}^*\omega_l + K\text{d}^*\tilde{\omega}_l} &= 2\hat{K}(\omega_{l1}^+ \omega_{l2}^+ + \omega_{l1}^- \omega_{l2}^-) + (1 + \hat{K}^2) \left[(\omega_{l1}^+)^2 (\omega_{l2}^+)^2 + (\omega_{l1}^-)^2 (\omega_{l2}^-)^2 \right] \\ &\quad + (1 - \hat{K}^2) \left[(\omega_{l1}^+)^2 (\omega_{l2}^-)^2 + (\omega_{l1}^-)^2 (\omega_{l2}^+)^2 \right] \end{aligned} \quad (38)$$

Finally for links contained in C_2 it is also straightforward to carry out the same type of expansion. These factors can be of two different types depending on the corresponding sign in the r.h.s. of (29) carried by the link in question. If the sign is positive we obtain

$$e^{K(d^*\omega_l - d^*\tilde{\omega}_l)} + e^{-K(d^*\omega_l - d^*\tilde{\omega}_l)} = 2(1 - \hat{K}^2) \left[(\omega_{l1}^+)^2 (\omega_{l2}^+)^2 + (\omega_{l1}^-)^2 (\omega_{l2}^-)^2 \right] + 2(1 + \hat{K}^2) \left[(\omega_{l1}^+)^2 (\omega_{l2}^-)^2 + (\omega_{l1}^-)^2 (\omega_{l2}^+)^2 \right] \quad (39)$$

For links with a minus sign the result is

$$e^{K(d^*\omega_l - d^*\tilde{\omega}_l)} - e^{-K(d^*\omega_l - d^*\tilde{\omega}_l)} = 4\hat{K}(\omega_{l1}^+\omega_{l2}^- + \omega_{l1}^-\omega_{l2}^+). \quad (40)$$

We are now ready to construct the “diagrams” of our expansion by choosing one term from each plaquette and link expansion in all possible ways consistent with the rule that eventually each plaquette has to carry an even power of either ω^+ or ω^- but not both. This constraint implies that the plaquettes carrying $(\theta^- \pm \hat{h}\theta^+)\omega^\pm$ are pairwise connected with stacks of links carrying an odd power of the ω^\pm 's. These links always come with an additional factor $\sim \hat{K}$ while links carrying an even power of the ω 's contain $1 \pm \hat{K}^2$. Recall that $\hat{K} = \tanh K$ is small at low temperature which means that a stack of odd ω -power links costs an energy proportional to its length. Moreover the plaquettes that are connected by these stacks carry vortices (θ^-) with a small mixing of the no-vortex state ($\sim \hat{h}\theta^+$). We can thus recover the familiar string vortex picture in this representation, the only subtlety being that the effective magnetic field gives a small mixing between θ^+ and θ^- .

After integrating out the ω variables, up to positive constant factors, each diagram has the form

$$D = \left\langle \prod_{p \in \bar{\Lambda}} (\theta_p^- \pm \hat{h}\theta_p^+) \prod_{p \notin \bar{\Lambda}} (\theta_p^+ \pm \hat{h}\theta_p^-) \right\rangle_L, \quad (41)$$

where $\langle \rangle_L$ means expectation with respect to the SO(3) measure $d\nu_+[U]$ and $\bar{\Lambda}$ is a subset of plaquettes containing an even number of plaquette